Increasing the penetration depth for ultrafast laser tissue ablation using glycerol based optical clearing

Ilan Gabay[a], Kaushik G. Subramanian[a], Chris Martin[b], Murat Yildirim[a], Valery V. Tuchin[c,d,e], and Adela Ben-Yakar[a,b]

[a]Department of Mechanical Engineering, The University of Texas at Austin, Austin, TX, USA
[b]Department of Biomedical Engineering, The University of Texas at Austin, Austin, TX, USA
[c]Research-Education Institute of Optics and Biophotonics, NG Chernyshevsky Saratov National Research State University, Russian Federation
[d]Interdisciplinary Laboratory of Biophotonics, Tomsk National Research State University, Russian Federation
[e]Laboratory of Laser Diagnostics of Technical and Living Systems, Institute of Precise Mechanics and Control RAS, Russian Federation

Abstract

Background: Deep tissue ablation is the next challenge in ultrafast laser microsurgery. By focusing ultrafast pulses below the tissue surface one can create an ablation void confined to the focal volume. However, pulse energies need to increase exponentially as the ablation depth increases due to tissue scattering. Optical clearing (OC) might reduce the intensity and increase the maximal ablation depth by lowering the refractive index mismatch, and therefore reducing scattering. In our previously proposed clinical goal we aim at creating superficial voids below the epithelium in scarred vocal folds to enable localization of injected biomaterials to bring back the tissue elasticity and restore phonation. In another application, our goal is to remove small lesions in delicate vocal folds by detaching them from tissue by ablating around them which ideally should start as deep as possible.

Materials and methods: Fresh porcine vocal folds were excised and subject to treatment with OC agent (75% glycerol). Collimated transmittance was monitored. The tissue was optically cleared and put under the microscope for ablation threshold measurements at different depths.

Results: The tissue optically cleared after approximately two hours of treatment. Fitting the ablation threshold measurements to an exponential decay graph indicated that the scattering length of the tissue increased to 83±16 μm, more than doubling the known scattering length for normal tissue.

Conclusion: Optical clearing with glycerol increases the tissue scattering length and therefore reduces the energy for ablation and increases the maximal ablation depth. This technique can potentially improve clinical microsurgery.

Keywords: Ultrafast laser, optical clearing, vocal folds, ablation, glycerol, microsurgery

1. Introduction

In recent years, ultrafast laser microsurgery has become a superior technique for ablation of tissues, cells, and subcellular structures [[1], [2]]. Their high peak intensity and short pulse duration lead to efficient and rapid ionization of the tissue before any substantial energy can be lost to heat diffusion, confining the ablation to the focal volume. As a result, the process requires much less energy for ablation and leads to significantly less heating of the surrounding tissue [[3]]. Ultrafast laser surgery has therefore become a clinical tool, especially in ophthalmology, where high precision subsurface ablation was reported in transparent biological materials such as the cornea [[4]]. More recently,

Dynamics and Fluctuations in Biomedical Photonics XIII, edited by Valery V. Tuchin, Kirill V. Larin, Martin J. Leahy, Ruikang K. Wang, Proc. of SPIE Vol. 9707, 97070X
 · doi: 10.1117/12.2213482

subsurface ablation of the sclera – a highly scattering tissue – was reported [[5]]. Impressive results in brain surgery were also shown, imaging and ablating at depths of hundreds of microns in rats *in vivo* [[6]].

Vocal fold (VF) scarring is one of the major causes for voice disorders and may arise from overuse or post-surgical wound healing. One promising treatment uses the injection of soft biomaterials to restore viscoelasticity of the outermost vibratory layer of the VF - superficial lamina propria. Ongoing development of such materials is a significant research focus in the field of phonosurgery [[7]]. A common unsolved problem facing the surgical use of injectable materials is their accurate and effective placement in a superficial plane inside scarred VF. Scared VF tissue is very dense and an effective method for injection and localization of the biomaterial is missing. Recently, we have proposed to localize biomaterials by ablating sub-epithelial voids using ultrafast laser pulses [[8],[9]]. Since then, we have successfully demonstrated the feasibility of this technique by localizing a polyethylene glycol (PEG) based biomaterial stained with Rhodamine dye into an ablated sub-epithelial void of 2x1 mm^2 in a scarred hamster cheek pouch *ex vivo* [[10]]. In a parallel effort, we have been developing fiber-based miniaturized probes for delivering ultrafast laser pulses for microsurgery and nonlinear imaging [[11], [12], [13]]. To guide such high-precision surgery in tissue, there is a need for imaging the location of the scarred tissue deep below the epithelium. Therefore, our ultimate goal is to create the sub-epithelial voids and image them at depths of hundreds of microns.

In scattering tissue, the mechanism causing multiple scattering is the refractive index mismatch between the tissue proteins, such as collagen, and the surrounding interstitial fluid. The scattered light does not contribute to nonlinear absorption in the focal volume. To increase the ablation depth in a scattering tissue, one can improve on the "laser side", and choose a wavelength for increased scattering lengths [[5]]. Another way to improve ablation depth is by moving from femtosecond pulses to the picosecond range to reduce high peak powers [[8], [9]].

The third approach, that can also be combined with the above mentioned improvements, is to alter the medium rather than the laser light by optical clearing (OC) using biocompatible chemical agents, which aims to increase scattering length at a given wavelength. The topical application of a chemical agent directly onto the surface of a highly scattering tissue specimen initiates two processes. The first one is the diffusion of the clearing agent into the tissue that is followed by the second process of the osmosis of the tissue fluid or dehydration. Effectively, the tissue fluid is partially displaced by the chemical agent, thereby reducing refractive index mismatch between tissue constituents and thereby reduce scattering [[14], [15]]. The use of glycerol as an OCA was very recently used *in vivo* to better understand the OC mechanism in a live tissue [[16]]. It was found that the presence of OCA affected the thickness of the tissue but not its organization.

A variety of optical clearing agents (OCAs) have been used, showing impressive reduction in tissue scattering. The use of Hypaque, for example, allowed subsurface ablation at depths up to 500 μm in highly scattering human sclera specimens, using a 1060 nm laser wavelength [[17]]. It is not mentioned, however, if the damage at the maximal depth was confined to the focal point. More recently, porcine skin optically cleared with glycerol, was ablated up to a depth of 1 mm [[18]]. However, the ablation site dimensions extended way beyond the focal volume dimensions and precision was diminished. Tissue optical clearing using mechanical compression was also recently demonstrated up to depth of 1.7 mm [[19]], but seemed to be limited only to superficial and flat body parts which might limit its wide clinical use.

A paper by Genina *et al.* thoroughly reviews the recent advance in OC in general, and more specifically in nonlinear imaging microscopy [[20]]. According to that review, two photon microscopy of human skin has improved imaging depth by 2-fold when using a glycerol based OCA up to a maximal imaging depth of 80 μm. SHG imaging was done on muscle tissue, also using glycerol. Quantitative data of the normalized SHG signal showed 2.5-fold improvement up to a depth of 210 μm. Other non-imaging methods such as integration sphere were used to determine the OC effect on the tissue and found up to 20 fold increase in scattering length [[21]]. These results do show promise for the use of glycerol based OC to reduce tissue scattering. Still there seems to be a high discrepancy which may stem from the fact that these methods are system specific in determining the tissue properties and maximal imaging depth. Imaging systems will show a different trend of the collected signal in response to OC, depending on whether they are

collecting forward or backward scattered light. The determination of the improvement in imaging depth would therefore be subjective. Having the OC technique heavily researched especially for improving imaging modalities, together with its being safe to work with in the clinic, motivated us to research the effect it will have on microsurgery, and specifically, on increasing the ablation depth inside a highly scattering tissue.

The current study evaluates the efficacy of a glycerol based solution as an OCA to increase the tissue scattering length in an effort to increase the ablation depth. We directly measure the scattering length of tissue before and after the application of the OCA using a modified and more general version of our previously proposed method for measuring extinction coefficient of tissue [[9]]. In this method we evaluate the scattering length by finding the surface energies needed to initiate tissue ablation at few depths and determined the scattering length using Beer's law. We hypothesized that ablation threshold experiments provide means for directly and objectively measuring the change in the tissue scattering length.

2. Experimental methods

Porcine trachea was obtained from a local slaughterhouse. The fresh tracheas were immediately brought to our lab. From each trachea we extracted two pairs of VF that were immersed in Phosphate Buffer Solution (PBS). For our experiment we used the inferior vocal fold. The OCA was prepared the night before the experiment by mixing glycerol and PBS to get 75% glycerol concentration, by volume. This concentration was previously found optimal in reducing the tissue scattering [[21]], while not inducing any structural change in the collagen fibers [[16]]. The mixed solution was stirred for 1 minute and left over night at room temperature. The tissue sample was either immersed in the OCA, for the ablation experiments, or a few drops were applied topically, for the collimated transmittance experiment.

To assess the improvement in tissue clarity over time, we measured collimated transmittance through the tissue, while a clearing agent was actively matching the refractive index inside the tissue. A mode locked Ti:sapphire laser (MaiTai, Newport), 0.4 W average power, 800 nm wavelength was aligned to normally incident on a petri-dish, and hit the 200 μm aperture of an optical fiber probe coupled to a spectrometer (Ocean Optics). A VF tissue sample, 4 x 4 mm^2 wide, 0.5 ± 0.1 mm thick was placed on the petri-dish, with the epithelial part facing the laser, and the initial transmittance was recorded. At that time, few drops of the OCA were applied on top of the tissue. The tissue transmittance was monitored over time to measure the time scale of changes in the tissue following the application of an OCA.

To measure the change in scattering length of the optically cleared tissue, we carried out a series of tissue ablation experiments on fresh VF samples. The samples were immersed in an OCA solution for 2 hours, after which it was visually examined. The tissue appeared to be much clearer than normal tissue but also stiffer and smaller in volume. The tissue was put inside a petri dish, this time with the epithelium facing the cover slip at the bottom of the petri dish. By gently pressing the tissue against the glass, we could ensure a continuous glass-tissue interface. We imaged the tissue using Third Harmonic Generation (THG) microscopy in our tabletop homebuilt nonlinear microscope[[22]], with an erbium-doped fiber laser (1.5 ps, 300 kHz, 1552 nm Discovery, Raydiance Inc.) as the excitation source while collecting the THG signal at 517 nm. Three photon process involved in THG imaging as well as the high penetration of the 1552 nm excitation wavelength enabled us to image the ablation results at deep locations immediately following the ablation [[23]]. This was a convenient characterization method since the histological examination of the tissue was difficult to implement. In general it is very hard to find the ablation locations formed at threshold fluences after the bubbles collapse within a few tens of seconds. The average excitation laser power on the sample ranged from tens to hundreds of milliwatts, depending on the imaging depth. In our previous studies we showed that one could avoid tissue heating due to increased absorption at 1550 nm excitation wavelengths by controlling the imaging times and letting tissue to cool in between the imaging planes [[23]]. Therefore we refrained from long exposure times, especially at deep locations, to avoid heating. The imaging system had the ability to zoom in from a 400 μm FOV, up to 40 μm FOV at its maximal magnification. The objective NA was 0.75 (20× air objective, Nikon Plan Apo) and the

corresponding spot size could resolve 1 μm features. Such imaging resolution was satisfactory in assessing the percentage of ablated area out of the whole FOV.

Ablation experiments were done on 3 different VF samples, at 5 different depths. Initially we found the glass-tissue interface, which was easily and most accurately detectable thanks to the high sensitivity of THG for refractive index change. The microscope was then focused deeper inside through the cells of the epithelium layer which spanned across approximately 60 μm depth, until collagen fibers were first observed. The microscope was then moved an additional 36, 60, 84, 108 or 132 μm deeper into the fibers of the lamina propria (LP) which was set as the ablation position, corresponding to a total depth of 96, 120, 144, 168 and 192 μm from the tissue surface. For ablation, we used a Ti:sapphire oscillator (Tsunami, Spectra-Physics) at a central wavelength of 804 nm and a repetition rate of 80 MHz to seed a regenerative amplifier (Spitfire, Spectra-Physics) to generate a train of high energy 250 fs pulses at 1 kHz. The $1/e^2$ spot radius on the tissue was measured to be w_0 = 0.7 μm. The ablating laser was co aligned with the imaging laser to have a matching FOV. We chose to ablate a 40 × 40 μm^2 for the threshold experiments. The low frequency of the ablating laser made it necessary to use a frame rate of 1/15 frames per second to get a full coverage of the FOV, with 18 overlapping pulses at each point. The tissue was translated 30 μm back and forth before and after the ablation to account for focal plane shift due to difference between the imaging and ablation wavelengths.

The experiments to assess the scattering length of the tissue followed a modified version of a new method that we recently developed [[9]]. In this method we are fitting our ablation threshold measurements to Beer's law in order to assess the tissue parameters. In each ablation experiment we adjusted the pulse energy and monitored the outcome. By imaging the entire volume of the ablation bubble we ensured to capture its maximal cross section and that the damage did not extent beyond the focal volume. In each depth, we ablated a few locations around the threshold fluence before moving to a different depth. We assumed that the threshold energy over the ablated region follows a t-distribution, mostly from variations in the scattering properties of the tissue and from slight variations in the ablation depth due to surface roughness. The extent of the ablation at a given depth as a function of the pulse energy can therefore be defined by a sigmoid function. For each depth we fitted a sigmoid curve to 5-10 measured points using Eq. (1), where each of our data points is given by the pulse energy E and the normalized ablation area (extent of ablation divided by the scanned FOV), given by $S(E)$.

$$S(E) = \frac{1}{1 + e^{-(E-E_{th})/\rho}} \tag{1}$$

We then extracted the threshold energy E_{th} which corresponds to the energy when 50% of the FOV was ablated, while the sigmoid width ρ gave us an estimation of the error.

The results of ablation threshold as a function of the depth inside the tissue were fitted to Eq. (2) based on Beer's law. This equation describes an exponential decay due to scattering by the epithelium layer followed by further scattering by the LP layer. We assume absorption at the ablation wavelength of 804 nm is negligible.

$$F_{th} = \frac{E_{surf}}{\pi w_0^2} e^{-\frac{z_{ep}}{l_{ep}} - \frac{z_{lp}}{l_{lp}}} \tag{2}$$

Here z_{ep} and l_{ep} are the thickness and scattering length of the epithelium layer, z_{lp} is the depth from the epithelium-LP interface to the focal point, and l_{lp} is the scattering length of the LP. F_{th} is the threshold fluence at the focal point being ablated, E_{surf} is a pulse energy at the tissue surface, and w_0 is the spot size at the focal point. The use of the exponential decay provided by Beer's law is suitable for the analysis here since the number of scattering events is small and the ablation depth is of the same scale as the scattering length [[24]].

3. Results and discussion

Figure 1 is showing a typical graph of the change in transmittance through the tissue as a function of time for a time interval of more than 2 hours. Our motivation with this measurement was to determine the optimal time after which scattering is substantially reduced while verifying that the time was short enough for keeping the tissue as fresh as possible. The graph shows an order of magnitude increase in transmittance, which is attributed to change in the scattering length of the tissue thanks to the increased refractive index matching. Since the tissue is thick, the process involves multiple scatterings and a simple Beer's law analysis becomes invalid. Another important conclusion from that graph is that the OC process is faster at the beginning, however, much slower after roughly 100 minutes. For clinical applications, one could use various drug delivery methods to reduce the time for OC from hours to minutes by adding DMSO to the OCA [[25]]. The general trend of fast increase in transmission is followed by a saturation after ~120-130 minutes as repeated in other samples. Some of the samples showed a dip in the curve, similar to that seen in Figure 1, around 120 minutes. The reason for that dip might be related to the dynamics of the OC process which involves diffusion and osmosis processes as explained before, and therefore might change the surface curvature and angle of incidence of the light, and affect alignment. Still, the general trend of increase in transmittance is clear from the graph. After having an estimate of the time scale in which the OCA is well diffused inside the tissue we were able to measure the resulting change in the tissue scattering length. As explained, we chose to measure the scattering length by preforming ablation threshold measurements.

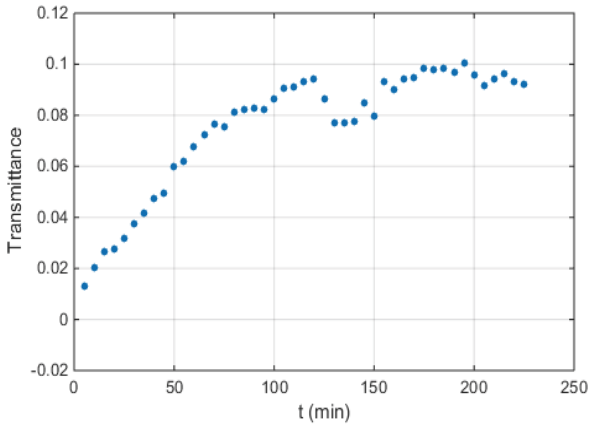

Figure 1: Collimated transmittance of 800 nm ultrafast laser light through an ex vivo porcine vocal fold as a function of time after a topical application of the optical clearing agent.

Figure 2 shows a typical ablation experiment results at 96 μm depth. The THG images in Figs. 2b and c show the collagen fiber bundles before and after ablation with a red dashed line indicating the targeted ablation FOV of 40 × 40 μm^2. Ablation with a 195 nJ pulse energy on the tissue surface was able to create a bubble covering 25% of the targeted FOV. The THG images correspond to the data point in Fig. 2a is marked with an arrow. Other data points were collected and fit to a sigmoid as shown in the plot. Similar graphs were obtained for all 5 depths.

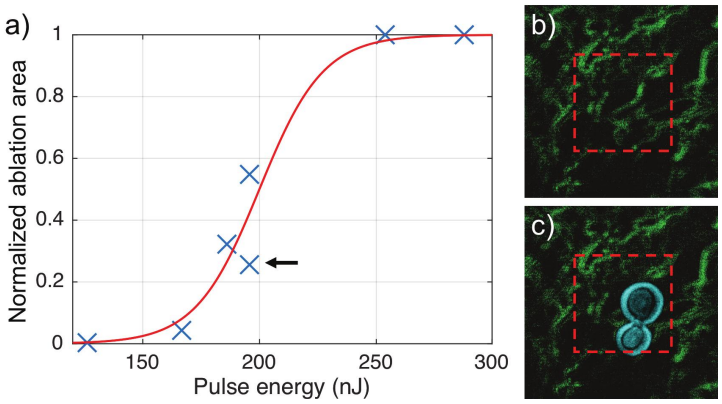

Figure 2: (a) The graph describes a set of measurements of the ablated area normalized with the targeted FOV when the laser was focused 96 μm deep inside the tissue (60 μm epithelium followed by 36 μm superficial lamina propria). The measurements were fit to a sigmoid curve to determine the energy at the surface that would ablate 1/e of the tissue in the FOV. (b,c) A 80 × 80 μm^2 imaging FOV out of which 40 × 40 μm^2 marked in a red dashed line is the ablation FOV. Fig. (b) is before ablation, showing the collagen fiber bundles in the tissue. (c) is after ablation. an ablation bubble is seen that was captured immediately after ablating the tissue with a 195 nJ pulse energy on the tissue surface. The ablated area covered 25% of the ablation FOV and that figure corresponds to one of the points in (a), denoted with an arrow.

Next, we analyzed the measurements of the ablation area for different pulse energies as we move across the sample. To properly present our date taken at different points with varying epithelium thickness, across the tissue we introduced z_{ep}^{avg}, which is the average epithelium thickness, into Eq. (2) and obtained Eq. (3) and, by taking the reciprocal, Eq. (4).

Equation (4) is describing the surface energy needed to initiate ablation at some depth $z = z_{ep}^{avg} + z_{lp}$ inside the LP layer. Previously we measured the scattering length of untreated epithelial and LP tissues as 35 ± 2.4 μm [[23]]. This value well agreed with the literature [[24]]. As explained before, the OC process displaces the tissue fluid with the OCA, and therefore the most dramatic change in tissue properties is inside the LP where molecules of tissue fluid and glycerol more free to move. The epithelium, on the other hand, does not undergo a dramatic change as found by Millon *et. al* [[26]]. We therefore assumed that OC had a small or no effect on the scattering length of the epithelium and focused our measurements in the properties of the LP. The tissue ablation threshold fluence F_{th} is specific per tissue type. We previously measured it in our setup and found to be 1.9 ± 0.1 J/cm^2 for the LP of the inferior VF [[27]]. Measured ablation threshold from 5 depths were fitted into an exponential decay curve according to Eq. (4).

$$\frac{F_{th} \cdot \pi w_0^2}{E_{surf} e^{\frac{z_{ep}^{avg} - z_{ep}}{l_{ep}}}} = e^{-\frac{z_{ep}^{avg}}{l_{ep}} - \frac{z_{lp}}{l_{lp}}} \tag{3}$$

$$\frac{E_{surf}}{F_{th} \cdot \pi w_0^2 e^{\frac{z_{ep}^{avg} - z_{ep}}{l_{ep}}}} = e^{\frac{z_{ep}^{avg}}{l_{ep}} + \frac{z_{lp}}{l_{lp}}} \tag{4}$$

Figure 3 shows the surface energy at the tissue surface as a function of the ablation depth as it is given by Eq. (4). The energy axis corresponds to the left hand side of Eq. (5) and represents the surface energy normalized by the threshold energy (its reciprocal is shown for simplicity). In the epithelial layer, the curves for optically cleared and normal tissue are assumed to consolidate due to the fact that the epithelium is not being optically cleared as mentioned before. When reaching the LP, our measurements show a big deviation from the assumed non-cleared tissue. According to our measurements, the scattering length of the optically cleared tissue has increased to 83 ± 16 μm, which is more than doubling the known scattering length for normal tissue.

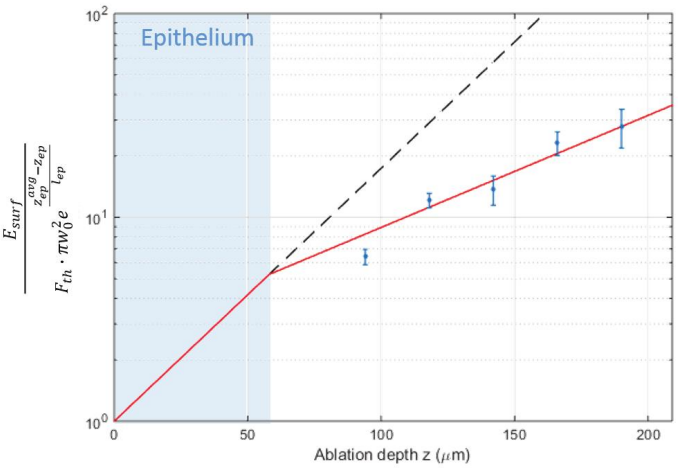

Figure 3: Surface energy as a function of the depth inside the tissue. The red line is for the optically cleared tissue. While in the epithelium, it has a scattering length of 35 μm, and when reaching the superficial lamina propria which was optically cleared, the measured scattering length increases to 83 ± 16 μm. The dashed line is an approximated curve for normal tissue

The graph also shows that we were able to create threshold ablation, which is an ablation void confined to the focal volume, at a depth of 196 μm. We do not have an experimental support but can carefully assume that reaching that depth is effectively equivalent to a much deeper point due to tissue shrinkage. Still, this result by itself is important since it describes an ablation void at threshold energy, almost 200 μm deep, which to our knowledge was not shown before for the same experimental conditions. It is also important to emphasize that theoretically, the optically cleared tissue with a scattering length of ~83 μm should allow us to ablate at much deeper locations. Our imaging system could not resolve the ablation bubble at depths larger than 200 μm because of the limited powers currently available by the laser source. Scientific literature for improved scattering length measurements after OC, shows high discrepancy. Some base their measurements on purely imaging depth experiments

reporting 2-4 fold improvement in imaging depth which is attributed to scattering length in a system specific manner [[20]], while others used integrating sphere measurements obtaining a 20 fold improvement without showing a corresponding substantial improvement in imaging depth [[21]]. The proposed method of measuring the scattering length by determining ablation threshold at different depths may provide a more quantitative and repeatable measurement method in determining the scattering properties of tissue.

4. Conclusion

In our study we first measured the time scale for tissue optical clearing of *ex vivo* porcine inferior vocal fold sample by a glycerol solution, and then we presented a set of measurements of tissue ablation threshold at different depths up to 196 μm. Our findings indicate that the optically cleared tissue scattering length increased more than 2-fold, from 35 ± 2.4 μm to 83 ± 16 μm and we can theoretically go much deeper, but are lacking an imaging system for those deep locations. Our conclusion is that optical clearing of tissues increases the ablation depth for a given laser pulse energy. As mentioned before, our clinical goal is to create subsurface voids in scarred VF and remove small lesions in delicate vocal folds. The next step will therefore be to perform *in vivo* experiments. The ability to show *in vivo* improvement in ablation depth with a biocompatible system is expected to bring forward many applications, especially in microsurgery.

Acknowledgements

This work was supported by a grant from Cancer Prevention Research Institute of Texas (CPRIT RP130412) VVT work was supported by grant No.14-15-00186 from the Russian Science Foundation

References

[1] A. Vogel, J. Noack, G. Hüttman, and G. Paltauf, "Mechanisms of femtosecond laser nanosurgery of cells and tissues," Appl. Phys. B 81, 1015-1047 (2005).

[2] S. H. Chung and E. Mazur, " Surgical applications of femtosecond lasers", J. Biophoton. 2, No. 10:557-572, (2009).

[3] A. A. Oraevsky, L. B. Da Silva, A. M. Rubenchik, M. D. Feit, M. E. Glinsky, M. D. Perry, B. Mammini, M. W. Small, and B. C. Stuart, "Plasma mediated ablation of biological tissues with nanosecond-tofemtosecond laser pulses: Relative role of linear and nonlinear absorption," IEEE J. Sel. Top. Quantum Electron. 2, 801-809 (1996).

[4] I. Ratkay-Traub, I. E. Ferincz, T. Juhasz, R. M. Kurtz, and R. R. Krueger, "First clinical results with the femtosecond neodynium-glass laser in refractive surgery," J. Refract. Surg. 19, 94-103 (2003).

[5] Z. S. Sacks, R. M. Kurtz, T Juhasz, G. Mourou, "Femtosecond subsurface photodisruption in scattering human tissues using long infrared wavelengths," Proc. SPIE Vol. 4241 (2001).

[6] J. Nguyen, J. Ferdman, M. Zhao, D. Huland, S. Saqqa, J. Ma N. Nishimura, T. H. Schwartz, C. B. Schaffer, "Sub-Surface, Micrometer-Scale Incisions Produced in Rodent Cortex using Tightly-Focused Femtosecond Laser Pulses," Las. Surg. Med. 43:382-391 (2011).

[7] S. M. Zeitels, A. Blitzer, R. E. Hillman and R. R. Anderson, "Foresight in laryngology and laryngeal surgery: a 2020 vision," Ann. Otol. Rhinol. Laryngol. Suppl. 198:2-16 (2007).

[8] C. L. Hoy, W. N. Everett, M. Yildirim, J. Kobler, S. M. Zeitels and A. Ben-Yakar, "Towards endoscopic ultrafast laser microsurgery of vocal folds," J. Biomed. Opt. 17(3), 038002 (2012).

[9] M. Yildirim, O. Ferhanoglu, J. Kobler, S. M. Zeitels and A. Ben-Yakar, "Parameters affecting ultrafast laser microsurgery of subepithelial voids for scar treatment in vocal folds," J. Biomed. Opt. 18(11), 118001 (2013).

[10] C. L. Hoy, O. Ferhanoglu, M. Yildirim, K. H. Kim, S. S. Karajanagi, K. M. C. Chan, J. Kobler, S. M. Zeitels and A. Ben-Yakar, "Clinical ultrafast laser surgery: recent advances and future directions," Journal of Selected Topics in Quantum Electronics 20(2), 1-14 (2014).
[11] C. L. Hoy, N. J. Durr, P. Y. Chen, W. Piyawattanametha, H. Ra, O. Solgaard and A. Ben-Yakar, "Miniaturized probe for femtosecond laser microsurgery and two-photon imaging," Optics Express 16(13), 9996-10005 (2008).
[12] C. L. Hoy, O. Ferhanoglu, M. Yildirim, W. Piyawattanametha, H. Ra, O. Solgaard and A. Ben-Yakar, "Optical design and imaging performance testing of a 9.6-mm diameter femtosecond laser microsurgery probe," Optics Express 19(11), 10536-10552 (2011).
[13] O. Ferhanoglu, M. Yildirim, K. Subramanian, and A. Ben-Yakar, "A 5-mm piezo-scanning fiber device for high speed ultrafast laser microsurgery," Biomed. Opt. Express 5(7), 2023–2036 (2014).
[14] V. V. Tuchin, "Optical clearing of tissues and blood using the immersion method," J. Phys. D Appl. Phys. 38(15): 2497–2518 (2005).
[15] A. K. Bui, R. A. McClure, J. Chang, C. Stoianovici, J. Hirshburg, A. T. Yeh, B. Choi, "Revisiting optical clearing with dimethyl sulfoxide (DMSO)," Lasers Surg. Med. 41(2):142–148, (2009).
[16] X. Wen, Z. Mao, Zh. Han, V. V. Tuchin, D. Zhu, "In vivo skin optical clearing by glycerol solutions: mechanism," J. Biophoton. 3(1–2), 44–52 (2010).
[17] Z. S. Sacks, R. M. Kurtz, T. Juhasz, G. A. Mourau, "High precision subsurface photodisruption in human sclera," J. Biomed. Opt 7(3):442–450, (2002).
[18] C. Tse, M. J. Zohdy, J. Y. Ye and M. O'Donnell, "Penetration and precision of subsurface photodisruption in porcine skin tissue with infrared femtosecond laser pulses," Trans. On Biomed. Eng., 55(3):1211-1218, (2008).
[19] J. Qiu, J. Neev, T. Wang, and T. E. Milner, "Deep subsurface cavities in skin utilizing mechanical optical clearing and femtosecond laser ablation," Las. Surg. Med, 45:383-390, (2013).
[20] E. A. Genina, A. N. Bashkatov, V. V. Tuchin, "Tissue optical immersion clearing," Expert Rev. Med. Devices, 7(6):825-42, (2010).
[21] R. LaComb, O. Nadiarnykh, S. Carey, P. J. Campagnola, "Quantitative second harmonic generation imaging and modeling of the optical clearing mechanism in striated muscle and tendon," J. Biomed. Opt., 13(2):021109, (2008).
[22] N. J. Durr, C. T. Weisspfennig, B. A. Holfeld, and A. Ben-Yakara, "Maximum imaging depth of two-photon autofluorescence microscopy in epithelial tissues", J. Biomed. Opt., 16(2):026008, (2011).
[23] M. Yildirim, N. Durr, A. Ben-Yakar, "Tripling the maximum imaging depth with third-harmonic generation microscopy," J. Biomed. Opt. 0001;20(9), 2015.
[24] S. L. Jacques, "Optical properties of biological tissues: a review," Physics in Medicine and Biology 58(11), (2013).
[25] D. Zhu, K. V. Larin, Q. Luo, V. V. Tuchin, "Recent progress in tissue optical clearing," Laser Photonics Rev. 7, No. 5, 732–757 (2013).
[26] S. R. Millon, K. M. Roldan-Perez, K. M. Riching, G. M. Palmer and N. Ramanujam, "Effect of optical clearing agents on the *in vivo* optical properties of squamous epithelial tissue," Las. Surg. Med., 38:920-7, (2006).
[27] C. Martin, A. Ben-Yakar, "Studying ultrafast laser parameters to deter self-focusing for deep tissue ablation," Photonics West Conference Proceedings 2016.
[28] V. V. Tuchin, "A clear vision for laser diagnostics (Review)," Journal of selected topics in quantum electronics, Vol. 13(6) (2007).